ISSN 1674-1056
http://cpb.iphy.ac.cn
http://iopscience.iop.org/cpb
中国物理 B
Chinese Physics
中国物理 Chinese Physics B

The structure and elasticity of phase B silicates under high pressure by first principles simulation

Lei Liu(刘雷), Li Yi(易丽), Hong Liu(刘红), Ying Li(李营), Chun-Qiang Zhuang(庄春强), Long-Xing Yang(杨龙星), Gui-Ping Liu(刘桂平)
Citation: Chin. Phys. B . 2018, 27(4): 047402. **doi:** 10.1088/1674-1056/27/4/047402

Journal homepage: http://cpb.iphy.ac.cn; http://iopscience.iop.org/cpb

What follows is a list of articles you may be interested in

High-pressure synchrotron x-ray diffraction and Raman spectroscopic study of plumbogummite

Duan Kang(康端), Xiang Wu(巫翔), Guan Yuan(袁冠), Sheng-Xuan Huang(黄圣轩), Jing-Jing Niu(牛菁菁), Jing Gao(高静), Shan Qin(秦善)
Chin. Phys. B . 2018, 27(1): 017402. **doi:** 10.1088/1674-1056/27/1/017402

Structural, elastic, and vibrational properties of phase H: A first-principles simulation

Chao-Jia Lv(吕超甲), Lei Liu(刘雷), Yang Gao(高阳), Hong Liu(刘红), Li Yi(易丽), Chun-Qiang Zhuang(庄春强), Ying Li(李营), Jian-Guo Du(杜建国)
Chin. Phys. B . 2017, 26(6): 067401. **doi:** 10.1088/1674-1056/26/6/067401

High-pressure dynamic, thermodynamic properties, and hardness of CdP_2

Shi-Quan Feng(冯世全), Ling-Li Wang(王伶俐), Xiao-Xu Jiang(姜晓旭), Hai-Nin Li(李海宁), Xin-Lu Cheng(程新路), Lei Su(苏磊)
Chin. Phys. B . 2017, 26(4): 046301. **doi:** 10.1088/1674-1056/26/4/046301

High-pressure studies on heavy fermion systems

Ye Chen(陈晔), Zongfa Weng(翁宗法), Smidman Michael, Xin Lu(路欣), Huiqiu Yuan(袁辉球)
Chin. Phys. B . 2016, 25(7): 077401. **doi:** 10.1088/1674-1056/25/7/077401

High-pressure Raman study of solid hydrogen up to 300 GPa

Xiaoli Huang(黄晓丽), Fangfei Li(李芳菲), Yanping Huang(黄艳萍), Gang Wu(吴刚), Xin Li(李鑫), Qiang Zhou(周强), Bingbing Liu(刘冰冰), Tian Cui(崔田)
Chin. Phys. B . 2016, 25(3): 037401. **doi:** 10.1088/1674-1056/25/3/037401

The structure and elasticity of phase B silicates under high pressure by first principles simulation*

Lei Liu(刘雷)[1,2,†], Li Yi(易丽)[1], Hong Liu(刘红)[1], Ying Li(李营)[1,2], Chun-Qiang Zhuang(庄春强)[3], Long-Xing Yang(杨龙星)[1], and Gui-Ping Liu(刘桂平)[1]

[1] *Key Laboratory of Earthquake Prediction, Institute of Earthquake Science, China Earthquake Administration, Beijing* 100036, *China*
[2] *National Key Laboratory of Shock Wave and Detonation Physics, Mianyang* 621000, *China*
[3] *Institute of Microstructure and Properties of Advanced Materials, Beijing University of Technology, Beijing* 100124, *China*

(Received 8 December 2017; revised manuscript received 13 January 2018; published online 10 March 2018)

The structures and elasticities of phase B silicates with different water and iron (Fe) content are obtained by first-principles simulation to understand the effects of water and Fe on their properties under high pressure. The lattice constants *a* and *b* decrease with increasing water content. On the contrary, *c* increases with increasing water content. On the other hand, the *b* and *c* decrease with increasing Fe content while *a* increases with increasing Fe content. The decrease of M (metal)–O octahedral volume is greater than the decrease of SiO polyhedral volume over the same pressure range. The density, bulk modulus and shear modulus of phase B increase with increasing Fe content and decrease with increasing water content. The compressional wave velocity (V_p) and shear wave velocity (V_s) of phase B decrease with increasing water and Fe content. The comparisons of density and wave velocity between phase B silicate and the Earth typical structure provide the evidence for understanding the formation of the X-discontinuity zone of the mantle.

Keywords: structural and elastic properties, phase B silicates, high pressure, first principles simulation

PACS: 74.25.nd, 63.20.dk, 62.50.–p **DOI:** 10.1088/1674-1056/27/4/047402

1. Introduction

Water and iron play important roles in the Earth evolution and dynamics because they have strong influences on the physical and chemical characters of minerals. Water can be transported into the Earth interior through hydrous minerals in subducting slabs.[1,2] As an important potential hydrous silicate phase, phase B (particular for hydrous phase B) was first identified by Ringwood and Major.[3] The phase B can be synthesized by heating a powder mixture of forsterite and periclase under hydrous conditions, above 15 GPa and 1500 °C, and will be decomposed into an assemble of liquid and periclase above its incongruent melting temperature (2300 °C at 23 GPa).[4] Akaogi and Akimoto[5] synthesized phase B with a crystal structure of $Mg_{23}Si_8O_{42}H_6$, and this structure was then revised into $Mg_{24}Si_8O_{42}H_4$ by Finger *et al.*[6] Studies about phase equilibrium in the system MgO–SiO_2–H_2O at 8.5 GPa–16 GPa and 750 °C–1200 °C showed dehydration of phase B might play an important role in the forming of the low-Q low-velocity zone in the depth about 300 km–500 km.[5] Finger *et al.*[7] described the details of crystallographic data of the phase B and anhydrous phase B (Anhy-PhB) that each SiO_6 octahedron shares all 12 edges with neighboring MgO_6 octahedra. A large number of edges shared among the octahedral make the high densities of the phase B and Anhy-PhB. The H bonding tends to increase, rather than reduce the structure density because all H bondings in phase B occurs within the humite-like layer, rather than between layers. The Anhy-PhB, which possesses the Mg end-member stoichiometry of $Mg_{14}Si_5O_{24}$, was first synthesized by Herzberg and Gasparik.[8] Ganguly and Frost[9] determined the stability of Anhy-PhB and the equilibrium boundary of the reaction forsterite + periclase = anhydrous phase B at 900 °C–1600 °C, and suggested that the reaction might lead to the formation of the X-discontinuity at 275 km–345 km depth in the subcontinental and subduction zone. High-pressure single crystal x-ray diffraction results of the Anhy-PhB at 7.3 GPa and room temperature show that the *c*-axis is most compressible (K_c = 137.3 GPa) and the *b* axis is least compressible (K_b = 175.4 GPa), and the rigid edge-sharing chains of MgO_6 and SiO_6 octahedra in the octahedral layer control its compressibility.[10] The thermochemical and -physical properties of the Anhy-PhB were simulated using hybrid B3LYP density functional theory from 0 to 20.3 GPa and the results are in agreement with the experimental data.[9–11] The partitioning of Fe into one of the six symmetrically distinct octahedral sites made the properties of Fe-bearing phase B $(Mg_{0.88}Fe_{0.12})14Si_5O_{24}$ (Fe-PhB), synthesized at 15 GPa and 1800 °C, remarkably different from those of phase B and the presence of Fe expands the stability of anhydrous phase B into the Earth's transition zone.[12] The properties of minerals under high pressure are important for understanding the structure and composition of the Earth. However, the research of the crystal structural and elastic properties of

*Project supported by the Science Fund from the Key Laboratory of Earthquake Prediction, Institute of Earthquake Science, China Earthquake Administration (Grant No. 2016IES010104) and the National Natural Science Foundation of China (Grant Nos. 41174071, 41273073, 41373060, and 41573121).

†Corresponding author. E-mail: liulei@cea-ies.ac.cn

© 2018 Chinese Physical Society and IOP Publishing Ltd

the phase B (including phase B, Anhy-PhB and Fe-PhB) under high pressure has been relatively rare. Only two results about crystal structures of Anhy-PbB were reported.[10,11] Theoretical simulations can establish a link between the experimentally observed peaks in the spectra and the underlying atomic dynamics and structure. First principles have been successfully applied to geosciences for understanding mineral properties of the crystal structure, elasticity, diffusion, melt, etc. under high pressure and temperature.[13–24] Differences among the different cases of phase B with different water and Fe content are important for understanding the effects of water and Fe content on mineral properties, the structure and composition of the mantle. Therefore, we investigate the crystal structural and elastic properties of Anhy-PhB, phase B, and Fe-PhB under high pressure by using first-principles calculations.

2. Simulation methods

The anhy-PhB and Fe-PhB are orthorhombic ($Pmcb$, $Z = 2$) phases with 43 atoms per unit cell. When Fe is present, it is positioned into one of the six symmetrically distinct octahedral sites, although it prefers the M3 position.[8] For the Fe atom, we did not calculate spin polarized. In contrast, the phase B crystallizes into the space group $P21/C$ ($Z = 4$) with 39 atoms per unit cell.[5] All the above phases involve the ordered intergrowth of two structural elements along the b-axis direction. One is a layered structure containing octahedrally coordinated Mg and tetrahedrally coordinated Si. The other is the layered structure only containing octahedrally coordinated Mg and Si.[6]

In this study, first-principles calculations are performed by using density functional theory[25,26] with the plane-wave pseudopotential. The calculations are implemented in the CASTEP code,[27] and the generalized gradient approximation (GGA) with PW91 parameterization[28] is used to describe exchange–correlation interactions. Ultrasoft pseudopotentials[29] are used to model electron–ion interactions with a plane-wave energy cutoff of 700 eV. A $3 \times 1 \times 2$ Monkhorst Pack grid of k-points is adopted for sampling the Brillouin zone. A convergence criterion of 5×10^{-7} a.u. for total energy is used in the self-consistent-field calculations.

The structures of the phase B at given pressures are calculated by simultaneously optimizing both atomic positions and lattice constants under Hellmann–Feynman forces and stresses acting on nuclei and lattice parameters, respectively.[30] The elastic constants are determined by stress–strain relations.[31] The magnitudes of all applied strains are 0.003 and the linear relation was ensured to be enough for this strain range.

3. Results and discussion

3.1. Benchmark calculation

To assess the performance of the total-energy density functional theory approach used here, we calculate the cell parameters and elastic constants of the Anhy-PhB, phase B, and Fe-PhB and compare them with the reported values (Table 1).

As shown in Table 1, the differences between the calculated lattice parameters and the reported values in previous studies are less than 2%, and the differences in volume are between 4% and 5%. The differences in elastic properties between our calculations and reported simulations and experiments are in a range of 4%–11.2%. These differences may be attributed to under-binding resulting from the use of the GGA in our calculations, in spite of differences in pressure and temperature. Our calculations are carried out at 0 GPa and 0 K, whereas the results reported in the literature were obtained under atmospheric conditions. Thermal and zero-point corrections to the elastic constants will very likely improve the agreement between the calculated and reported results. The general agreement of our calculations with previous results demonstrates the validity of our computational method and its ability to reproduce the properties of the phase B.

Table 1. Structural and elastic constants of phase B.

Phase	Lattice constants				Elastic modulus		Reference
	a/Å	b/Å	c/Å	V/Å^3	K/(GPa)	G/GPa	
Anhy-PhB $Mg_{14}Si_5O_{24}$	5.914	14.299	10.142	857.6	155.0	103.9	[11]
	5.875	14.194	10.059	838.8			[10]
	5.868	14.178	10.048	836.0			[6]
	5.978	14.414	10.231	881.5	139.4	92.3	this study
Δ	1.5%	1.3%	1.4%	4.2%	10.1%	11.2%	
Phase B $Mg_{12}Si_4O_{19}(OH)_2$	10.588	14.097	10.073	1458.4			[6]
	10.599	14.109	10.082	1462.4			[32]
	10.787	14.316	10.255	1536.2	136.4	88.1	this study
Δ	1.8%	1.5%	1.7%	4.9%			
Fe-PhB $(Fe_{0.12}Mg_{0.88})_{14}Si_5O_{24}$	5.908	14.241	10.069	847.2	142.6		[12]
$Mg_{9.4}Fe_{0.4}Si_{3.1}O_{14}(OH)_4$						[10]	
$(Fe_{0.14}Mg_{0.86})_{14}Si_5O_{24}$	5.979	14.298	10.081	812.5	149.1	96.3	this study
Δ	1.2%	0.4%	0.1%	−4.3%	4.3%		

Note: Δ denotes the difference between the result in this study and the mean of previously reported results.

3.2. Crystal structure under high pressure

Lattice constants (a, b, and c) of the phase B are calculated from 0 GPa to 30 GPa (Fig. 1). The results of previous studies are also included in Fig. 1. Both the previously calculated results[11] and our calculations are lower than experimental values.[10] As mentioned above, the calculated lattice constants in this study are generally lower than the previously reported values, which is primarily because of under-binding resulting from the use of the GGA in our calculations. Although the calculated lattice parameters are lower than the experimental data, the calculated change trends in lattice constants with pressure are consistent with the previous results.

The lattice constants a and b decrease with increasing water content, on the contrary c increases with increasing water content. The lattice constants b and c decrease with increasing Fe content, on the contrary a increases with increasing Fe content. Different occurrences of H and Fe atoms in crystal structure of the phase B lead to those different effects.

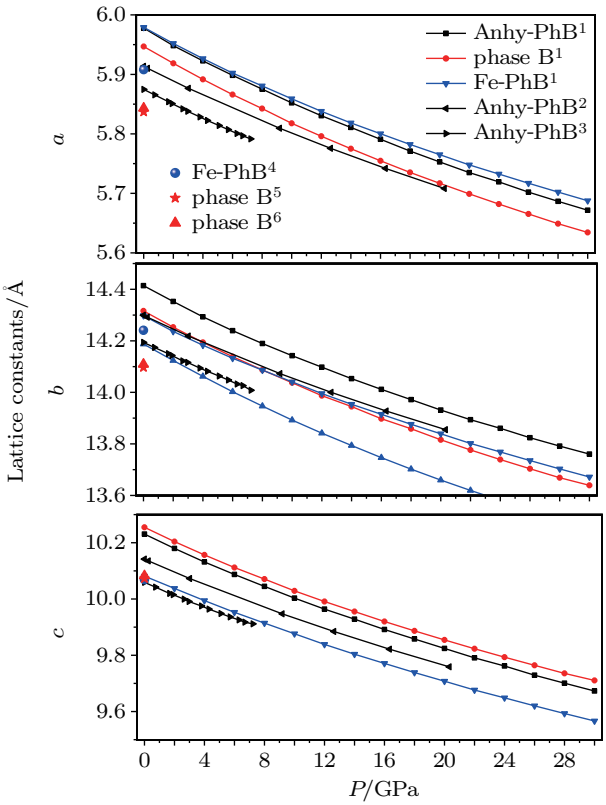


Fig. 1. (color online) Lattice constants of phase B varying with pressure (P). Different results are indicated by superscript numbers as follows: 1: this study; 2: Ottonello *et al.*[11]; 3: Crichton *et al.*;[10] 4: Hazen *et al.*;[12] 5: Finger *et al.*;[6] 6-Crichton *et al.*[32]

The changes of lattice parameters (e.g., bond length, bond angle, and polyhedral volume) with pressure are important for understanding mineral properties under high pressure. Because there are several different Si–O tetrahedra/octahedra along with M(Mg/Fe)–O octahedra in phase B, the lengths of Si–O and M–O bonds differ from each other within individual phases, but the differences are very slight. Therefore, we calculate the mean Si–O bond distance and M–O bond distance in each phase B. Hereafter, the calculated bond lengths in this study refer to these mean values.

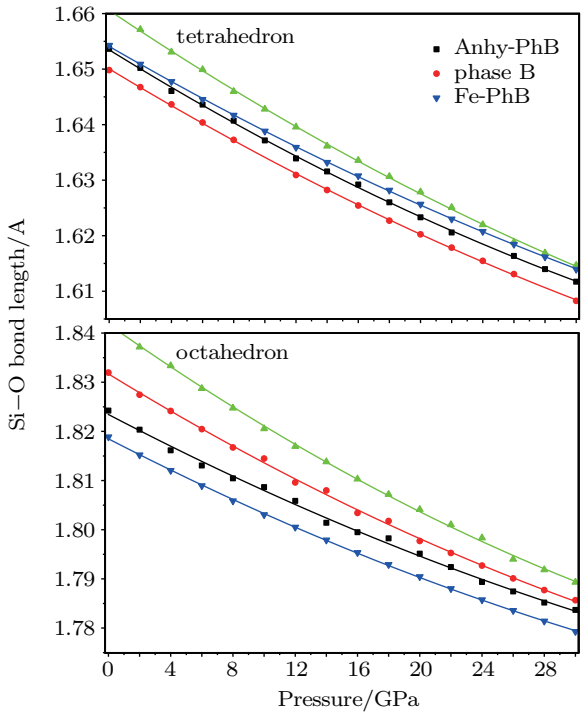


Fig. 2. (color online) Lengths of Si–O bond of phase B as a function of pressure.

The lengths of Si–O bond of a tetrahedron are shorter than those of an octahedron (Fig. 2). Water and Fe have opposite effects on the length of Si–O bond in octahedron and tetrahedron. The length of Si–O bond in the tetrahedron decreases with increasing water content and increases with increasing Fe content. However, the length of Si–O bond in the octahedron increases with increasing water content and decreases with increasing Fe content. The variations of SiO tetrahedral and octahedral volume with water and Fe contents coincide with the behavior of Si–O bond length. The SiO polyhedral volumes of Anhy-PhB, phase B, and Fe-PhB decrease by 6.5%, 7.4%, and 6.4% for tetrahedron and 7.5%, 7.4%, and 7.2% for octahedron as the pressure increases from 0 GPa to 30 GPa, respectively. Thus, the compression of the SiO tetrahedron is a little more than that of the SiO octahedron.

Metal(Fe/Mg)–O (MO) octahedron plays an important part in the crystal structure of phase B. The M–O octahedral bond distances of the phase Bs are shown as a function of pressure in Fig. 3. The lengths of Fe–O bonds are far shorter than those of Mg–O bonds. The lengths of Mg–O bonds increase with increasing water content and decrease with increasing Fe content. The volumes of the MgO octahedron in Anhy-PhB, phase B, and Fe-PhB decrease by 12.7%, 12.8%, and 12.6%, respectively, as the pressure increases from 0 GPa to 30 GPa.

The volume of FeO octahedron decreases by 11.3% over the same pressure range. Thus, the decrease of MO octahedral volume is greater than the decrease of SiO polyhedral volume under the same pressure range.

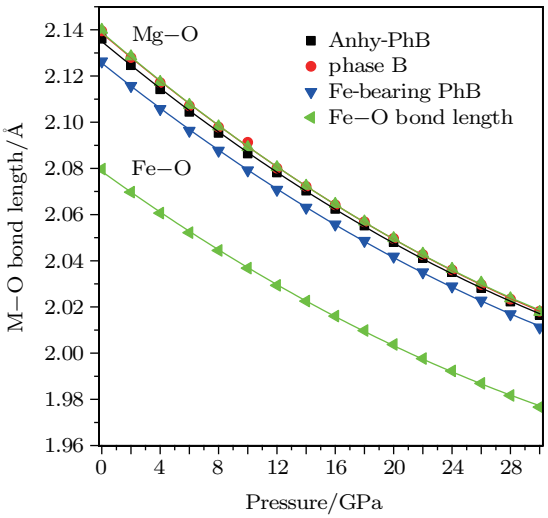


Fig. 3. (color online) Lengths of M–O bond of phase B as a function of pressure.

The densities of the phase B and typical Earth density structure are shown in Fig. 4. The density of Fe-PhB is 9.2% higher than that of Anhy-PhB, whereas those of phase B are 1.4% lower than that of Anhy-PhB. Thus, the density of phase B increases with increasing Fe content and reducing water content because of changes of volume and mass caused by H and Fe atom occupation or substitution in phase B crystal structure. These results are consistent with the changes of forsterite density with Fe and water contents.[33,34]

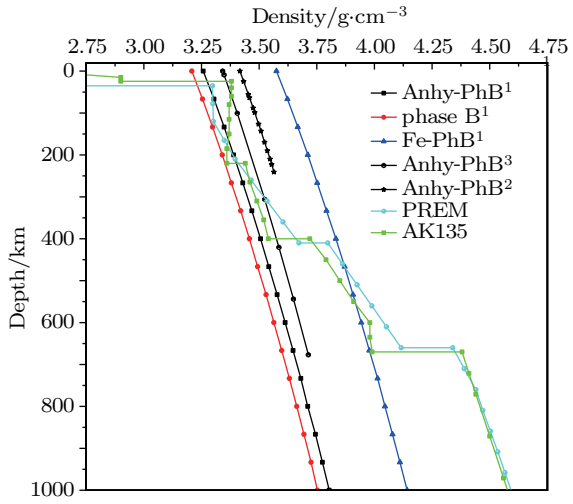


Fig. 4. (color online) Densities of phase B along the Earth's typical density structure. The different results are indicated by superscript numbers as follows: 1: This study; 2: Ottonello *et al.* 2010;[11] 3: Crichton *et al.* 1999.[10]

The densities of Anhy-PhB and phase B are close to the Earth density structure at depths of ∼ 50 km–410 km. However, the density of Fe-PhB is much higher than the Earth density within this depth range. The deeper the depth in the Earth (∼ 410 km–670 km), the closer to the Earth density the density of Fe-PhB becomes. However densities of the phase B and Anhy-PhB become smaller than the Earth density. The formation of Anhy-PhB by the reaction between forsterite and periclase may be responsible for the X-discontinuity at ∼ 260 km–330 km depth of the mantle.[9] The densities of the phase B in this depth range are close to the Earth density, which gives evidence for the formation of X-discontinuity at the mantle.

3.3. Elastic properties

The elastic parameters of minerals and their dependence on pressure are important in the Earth science because these properties are related to geophysical properties (e.g., seismic velocity and Poisson's ratio).

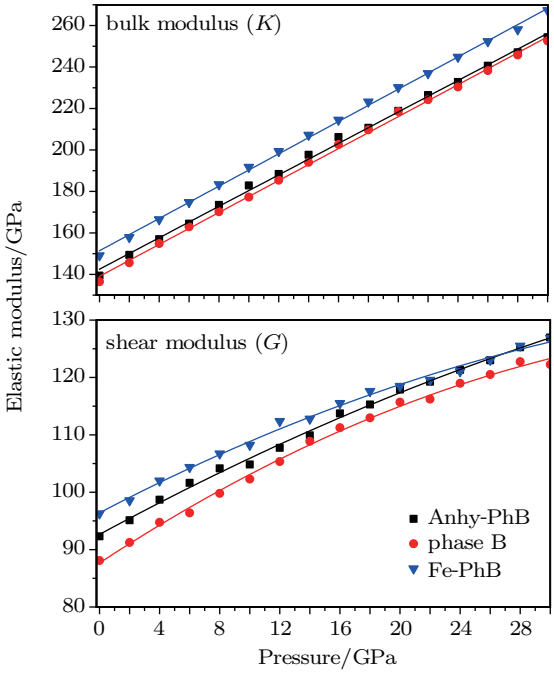


Fig. 5. (color online) Bulk and shear moduli of phase Bs as a function of pressure.

The bulk modulus (K) and shear modulus (G) increase with increasing Fe content and decrease with increasing water content (Fig. 5). The pressure derivatives of the bulk modulus, K', are directly calculated from the pressure dependence of K, yielding 3.79, 3.85, and 3.89 for Anhy-PhB, phase B, and Fe-PhB, respectively. The calculated K' values increase with increasing Fe and water content. The pressure derivatives of shear modulus (G') are directly calculated from the pressure dependence of G, yielding 1.42, 1.72, and 1.37 for Anhy-PhB, phase B and Fe-PhB, respectively. The G' increases with increasing water content and decreases with increasing Fe content.

The effects of the Fe and water content on the elastic modulus of phase B presented herein are consistent with the general trends in elastic behavior with water and Fe contents of

minerals changing.[33,35–37] For better understanding the elastic properties of phase B under high pressure and the effects of water and Fe, the 9 main elastic constants of the three cases of phase B are also listed as supplementary in Table 1.

3.4. Wave velocity

The wave velocity of a mineral is an important parameter for investigating the composition of deep Earth via comparison with the wave velocity structure of the Earth. The wave velocities for different cases of phase B under high pressure are plotted along with the typical Earth velocity structure in Fig. 6. The compressional wave velocity (V_p) and shear wave velocity (V_s) of phase B decrease with increasing water and Fe content. The sound velocities of hydrous and Fe-bearing (Mg, Fe, H)$_2$SiO$_4$ olivine are also lower than that of the Mg end member.[33,34] Previous first-principles calculations[38] and experimental studies[39] demonstrated that the sound velocity of Fe-bearing (Mg, Fe)SiO$_3$ perovskite is slightly (several percent) lower than that of the MgSiO$_3$ end member. Thus, the changes of wave velocities of phase B with water and Fe content presented from our simulations are consistent with previous results. The difference in velocity between hydrous and anhydrous lithology is useful in the remote sensing of water.[40,41]

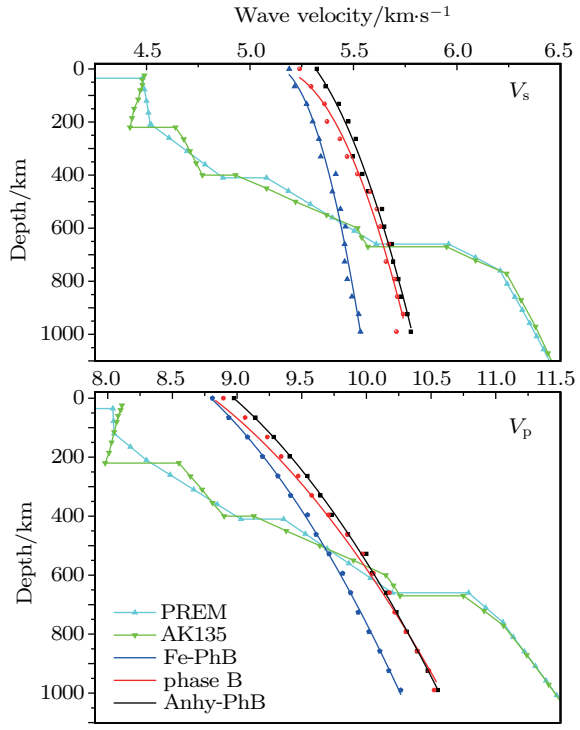


Fig. 6. (color online) Plots of the Earth depth versus wave velocity (V_s and V_p) for different cases of phase B.

The compressional and shear wave velocities of the phase B are higher than the Earth's velocity where the depths are less than about 450 km and 550 km, respectively. Then the velocities of the phase B become close to the Earth velocity at which depths are from about 550 km to 670 km. Phase B is thought to be stable at the depth of the mantle transition zone.[4] The formation of anhydrous phase B by the reaction between forsterite and periclase may be responsible for the X-discontinuity at $\sim$ 260 km–330 km depth of the mantle.[9] At the same time, the wave velocities of phase B are higher than those of olivine/forsterite.[42–44] So our results provide evidence for the stability zone and the formation of an X-discontinuity zone of the mantle.

4. Conclusions

The different ways for Fe and water atoms to occur in phase B structure (Fe occurs in phase B structure by substituting Mg, and H occurs within the humite-like layer of phase B), make different effects of water and Fe on lattice constants. The result helps to understand the influence mechanisms of water and Fe on properties of minerals. The decrease of M–O octahedral volume is greater than the decrease of SiO polyhedral volume over the same pressure range. The bulk modulus and shear modulus increase with increasing Fe content but decrease with increasing water content. The compressional wave velocity and shear wave velocity of phase B decrease with increasing water and Fe content. The results of density and wave velocity of phase B provide evidence for understanding the formation of the X-discontinuity zone of the mantle. However, the behaviors of phase B with different water or Fe content at high temperature need further investigating.

References

[1] Pearson D G, *et al*. 2014 *Nature* **507** 221
[2] Nishi M, *et al*. 2014 *Nat. Geosci.* **7** 224
[3] Ringwood A E and Major A 1967 *Earth Planet. Sci. Lett.* **2** 130
[4] Kato T and Kumazaw M 1985 *Geophys. Res. Lett.* **12** 534
[5] Akaogi M and Akimoto S 1980 *J. Geophys. Res.* **85** 6944
[6] Finger L W, *et al*. 1991 *Am. Mineral.* **76** 1
[7] Finger L W, *et al*. 1989 *Nature* **341** 140
[8] Herzberg C H and Gasparik T 1989 *Eos Trans.* **70** 484
[9] Ganguly J and Frost D J 2006 *J. Geophys. Res.* **111** B06203
[10] Crichton W A, Ross N L and Gasparik T 1999 *Phys. Chem. Minerals* **26** 570
[11] Ottonello G, *et al*. 2010 *Am. Mineral.* **95** 563
[12] Hazen R M, Finger L W and Ko J 1992 *Am. Mineral.* **77** 217
[13] Gillan M J, *et al*. 2006 *Rep. Prog. Phys.* **69** 2365
[14] Jahn S and Kowalski P 2014 *Reviews in Mineralogy & Geochemistry* **781** 691
[15] Zhang P, Kong C and Zheng C 2015 *Chin. Phys. B* **24** 024221
[16] Wei Z, Zhai D and Shao X H 2015 *Chin. Phys. B* **24** 043102
[17] Liu L, *et al*. 2015 *Chin. Phys. B* **24** 127401
[18] Lv C J, *et al*. 2017 *Chin. Phys. B* **26** 067401
[19] Karki B B 2015 *Phys. Earth Planet. Inter.* **240** 43
[20] Sun W D, *et al*. 2017 *Chem. Geology* in press
[21] Wu Zh and Wentzcovitch R M 2017 *Earth Planet. Sci. Lett.* **457** 359
[22] Zhang S, *et al*. 2016 *Earth Planet. Sci. Lett.* **434** 264
[23] Umeoto K, *et al*. 2017 *Earth Planet. Sci. Lett.* **478** 40
[24] Liu X H, *et al*. 2017 *Geochimica et Cosmochimica Acta* in press
[25] Hohenberg P and Kohn W. 1964 *Phys. Rev. B* **136** 864
[26] Kohn W and Sham L J 1965 *Phys. Rev. A* **140** 1133

[27] Clark S J, *et al*. 2005 *Zeitschrift für Kristallographie* **220** 567
[28] Perdew J P, *et al*. 1992 *Phys. Rev. B* **46** 6671
[29] Vanderbilt D. 1990 *Phys. Rev. B* **41** 7892
[30] Nielsen O H and Martin R M 1983 *Phys. Rev. Lett.* **50** 697
[31] Karki B B, Stixrude L and Wentzcovitch R M 2001 *Rev. Geophys.* **39** 507
[32] Crichton W A and Ross N L 2000 *Proceedings of AIRAPT*-17, Universities Press, Hyderabad, India, 2000
[33] Liu L, *et al*. 2009 *Phys. Earth Planet. Inter.* **176** 89
[34] Liu L, *et al* 2010 *J. Phys. Chem. Solids* **71** 1094
[35] Sanchez-Valle C, *et al*. 2008 *Phys. Earth Planet. Inter.* **170** 229
[36] Angel R J, *et al*. 2001 *Phys. Earth Planet. Inter.* **127** 181
[37] Jacobsen S D, *et al*. 2008 *Geophys. Res. Lett.* **35** L14303
[38] Kiefer B, *et al*. 2002 *Geophys. Res. Lett.* **29**
[39] Chantel J 2012 *Geophys. Res. Lett.* **39** L19307
[40] Abers G A 2000 *Earth Planet. Sci. Lett.* **176** 323
[41] Kawakatsu H and Watada S 2007 *Science* **316** 1468
[42] Zha C S, *et al*. 1996 *J. Geophys. Res.* **101** 17535
[43] Abramson E H, *et al*. 1997 *J. Geophys. Res.* **102** 12253
[44] Mao Z, *et al*. 2010 *Earth Planet. Sci. Lett.* **293** 250